Distributed Differential Evolution for Joint Power–Rate Control in Interference-Limited Cognitive Radio Networks

Nabin Keshav Gautam[1] **and Pramita Laxmi Shrestha**[2]
[1] Department of Computer Science and Engineering, Mid-West University,, 74 Birendranagar–Uttarganga Road, Surkhet 21703, Nepal
[2]Department of Computer Science and Engineering, Far Western University,, 21 Dhangadhi–Hasuliya Avenue, Kailali 10900, Nepal

ABSTRACT Cognitive radio networks allow secondary systems to access licensed spectrum under the condition that harmful interference to primary systems is avoided. In interference-limited deployments, the key performance determinants are the transmission powers and coding rates selected by secondary users, which jointly shape the experienced interference pattern and achievable throughput. Joint power and rate control in such environments is typically modeled as a coupled, nonconvex optimization problem with stringent interference constraints toward primary receivers and, in some cases, quality-of-service requirements for secondary links. Centralized solutions to this problem usually require global channel state information and tight coordination, which may be difficult to realize in large-scale or infrastructure-less networks. Distributed metaheuristic approaches offer an alternative by leveraging local computations and limited message exchange, at the cost of approximate optimality. This work examines a distributed differential evolution scheme tailored to joint power and rate control in interference-limited cognitive radio networks. The design focuses on linear constraint representations of interference coupling, a power-feasible encoding of individuals, and neighborhood-based information exchange. The resulting scheme aims to respect primary interference limits and secondary power budgets while exploring feasible tradeoffs between spectral efficiency and interference. Numerical investigations are described for multiuser scenarios with heterogeneous link budgets and channel conditions. The behavior of the distributed evolutionary dynamics is discussed with respect to convergence, robustness to initialization, and communication overhead. The study emphasizes structural aspects of the formulation and algorithm rather than specific system gains, with an aim to clarify the interplay between linear interference models and population-based distributed optimization.

KEYWORDS

1. Introduction

Cognitive radio networks are considered for scenarios in which unlicensed secondary users share spectrum with licensed primary users under carefully regulated interference conditions [1]. The need to exploit spectrum more efficiently has motivated mechanisms where secondary users opportunistically access spectrum while controlling the interference they produce toward primary receivers. In many practical deployments, especially in dense environments with aggressive frequency reuse, the dominant performance limitations arise from interference rather than thermal noise. In such interference-limited cognitive radio networks, link performance strongly depends on the joint configuration of transmit powers and coding rates across all active

Article info:
Nabin Keshav Gautam and Pramita Laxmi Shrestha. *Distributed Differential Evolution for Joint Power–Rate Control in Interference-Limited Cognitive Radio Networks*. Grovesocieties .

secondary users.

Traditional resource allocation methods for these networks often decouple power control and rate adaptation. Power control is responsible for shaping the interference pattern through appropriate transmit power selection, while rate adaptation chooses modulation and coding schemes consistent with the experienced signal-to-interference-plus-noise ratios [2]. When these two dimensions are optimized sequentially, the resulting configuration may not fully exploit the interference budget of primary links or the potential spatial reuse among secondary links. Joint optimization of power and rate can, in principle, capture the coupling between these decisions and expose additional operating points that balance throughput and interference.

However, joint power–rate control in interference-limited cognitive radio networks is typically accompanied by complex constraints. Secondary users must respect individual maximum power constraints originating from hardware or regulatory limits. They must also satisfy interference constraints at primary receivers, which are functions of the aggregate power transmitted by all secondary nodes weighted by their interference channel gains [3]. Furthermore, target quality-of-service constraints such as minimum rate requirements can introduce additional coupling across users through the interference structure. The resulting optimization problems are usually nonconvex and do not admit closed-form solutions in general configurations.

Centralized optimization techniques can be applied when a central entity has access to global channel state information and can compute the joint resource allocation before disseminating it to the network. This approach may be reasonable for small networks or slowly varying environments, but it becomes less suitable as the number of users grows or as channels and traffic loads fluctuate rapidly. The communication overhead required to collect channel information and to distribute updated allocations can be high, and the central node represents a single point of failure [4]. These considerations motivate distributed techniques, where each secondary user performs local computations based on partial information and limited message exchange with neighbors or a low-complexity control plane.

Metaheuristic approaches such as evolutionary algorithms have been investigated as flexible tools to address complex resource allocation problems without relying on detailed structural convexity. Differential evolution is an example of a population-based algorithm designed to search continuous parameter spaces through mutation and recombination of candidate solutions. Its operations are relatively simple and amenable to parallel or distributed execution. In the context of cognitive radio networks, a differential evolution algorithm can represent candidate joint power–rate vectors and iteratively refine them by evaluating an objective function that quantifies network performance under interference constraints [5].

A distributed realization of differential evolution requires a careful mapping of algorithmic primitives to local operations at individual secondary users. Each user can hold local representations of candidate solutions and evaluate local parts of the global objective using its measured or estimated channel state information. Exchanging population members or their evaluations across the network introduces communication overhead that must be controlled, particularly in interference-limited systems where control traffic itself may be subject to spectrum access constraints. Additionally, the evolutionary operations must incorporate feasibility handling with respect to power and interference constraints to avoid exploring large infeasible regions.

This work considers a distributed differential evolution scheme tailored for joint power–rate control in interference-limited cognitive radio networks [6]. The network model captures multiple secondary transmitter–receiver pairs sharing spectrum with one or more primary receivers. Each secondary user selects a transmit power level and an associated rate from a continuous or discretized admissible set. The resulting configuration induces interference at secondary and primary receivers according to given channel gains. The objective of the joint control problem is defined in terms of aggregate secondary rate with possible fairness weights, subject to power and interference constraints. The problem structure is expressed using linear interference coupling relations, providing a foundation for feasibility enforcement within the evolutionary search [7].

The paper develops a representation of individuals that encodes feasible or easily projectable power and rate vectors, discusses mutation and crossover operations compatible with distributed implementation, and introduces a selection rule that respects local information while approximating global objectives. The distributed scheme is described under the assumption of limited message exchange among neighboring nodes or via a lightweight signaling channel. The behavior of the algorithm is examined qualitatively with respect to convergence tendencies, sensitivity to parameter settings, and robustness to channel variability. Numerical examples are outlined for heterogeneous network scenarios with varying interference patterns. The discussion emphasizes how linear models of interference and rate feasibility can support the design of distributed evolutionary algorithms for cognitive radio resource allocation [8].

2. System Model and Assumptions

Consider a cognitive radio network consisting of a set of secondary transmitter–receiver pairs sharing spectrum with a set of primary receivers. Let the number of secondary links be denoted by an integer that can be indexed through symbols without explicit numerical values in the formulation. Each secondary transmitter communicates with its intended receiver over a common frequency band, leading to mutual interference among secondary links as well as interference toward primary receivers. The propagation conditions between each pair of nodes are represented by channel power gains that embed large-scale path loss and small-scale fading.

For each secondary link, a real nonnegative transmit power variable is defined. The transmit power for link index i is denoted by a scalar that must lie between zero and an upper bound associated with that link [9]. The upper bound models the maximum allowable transmit power imposed by hardware limitations or regulations. The received signal at the secondary receiver associated with link i is affected by the desired signal from its corresponding transmitter and by interference from all other

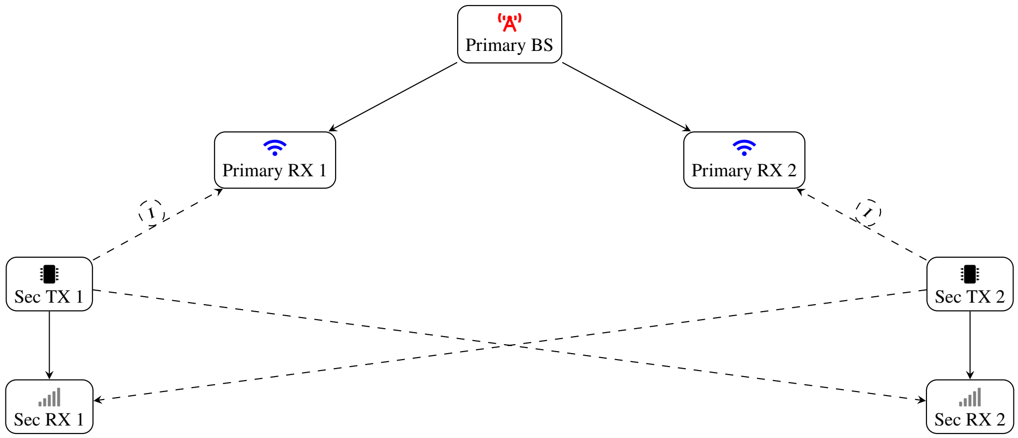

Figure 1 Cognitive radio network with primary infrastructure and secondary transmitter–receiver pairs creating mutual interference and aggregate interference at primary receivers.

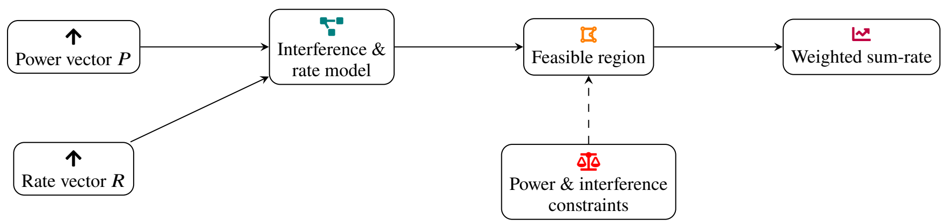

Figure 2 Functional decomposition of joint power–rate optimization, from decision variables through interference and rate modeling to feasibility evaluation and aggregate performance.

secondary transmitters. In addition, the receiver experiences noise, which is modeled as additive with a given variance.

Let h_{ii} denote the channel power gain from the transmitter of link i to its intended receiver. For any pair of distinct links i and j, let h_{ji} represent the channel power gain from the transmitter of link j to the receiver of link i. These gains are assumed to be known locally at the corresponding receivers, for example through pilot-based estimation. The interference perceived at secondary receiver i due to other secondary transmitters is described by linear superposition of their transmit powers weighted by the corresponding channel gains [10]. Under these assumptions, the instantaneous signal-to-interference-plus-noise ratio at secondary receiver i is given by a rational function of the power vector.

To express this relation, consider the following equation where all quantities are nonnegative:

$$\mathrm{SINR}_i \quad = \quad \frac{P_i h_{ii}}{\sum_{j \neq i} P_j h_{ji} + \sigma_i + I_i^P}. \tag{1}$$

Here P_i denotes the transmit power of link i, σ_i is the noise power at receiver i, and I_i^P models interference from primary transmitters toward secondary receiver i. The sum in the denominator captures the interference contribution from all other secondary transmitters. This relation is valid under standard assumptions of linear receivers and Gaussian noise [11].

Primary receivers are subject to interference from all secondary transmitters. For each primary receiver indexed by m, let g_{im} denote the channel power gain from the transmitter of secondary link i to primary receiver m. Each primary receiver is assumed to tolerate interference up to a specified threshold Q_m. This requirement is modeled by the linear constraint

$$\sum_i g_{im} P_i \quad \leq \quad Q_m \tag{2}$$

for each primary index m [12]. The sum extends over all secondary links that interfere with primary receiver m. This linear relation expresses the aggregate interference coupling from secondary transmitters toward each primary receiver.

Secondary links adapt their rates by choosing appropriate modulation and coding schemes. For each secondary link i, let R_i denote the spectral efficiency in bits per second per Hertz. This variable is treated as continuous in the system-level formulation, while in implementation it may represent a discrete set of supported modulation and coding combinations [13]. The mapping between R_i and the required signal-to-interference-plus-noise ratio at receiver i is characterized by a function derived from the modulation and coding performance. A commonly used approximation associates to each rate R_i a required threshold denoted by $\gamma_i(R_i)$, such that reliable communication at rate R_i is deemed feasible if the realized signal-to-interference-plus-noise ratio satisfies

$$\mathrm{SINR}_i \quad \geq \quad \gamma_i(R_i). \tag{3}$$

The function $\gamma_i(\cdot)$ can be modeled through analytical approximations or empirical curves derived from link-level simulation.

The rate feasibility constraint introduces a coupling between the transmit power vector and the rates [14]. Substituting the expression for SINR_i into the inequality above yields a linear inequality in the transmit powers once the rate R_i and the

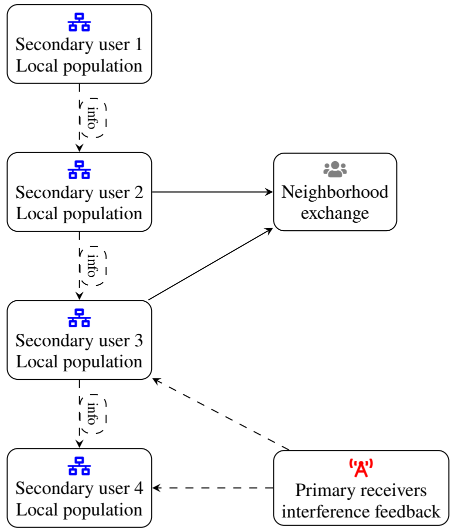

Figure 3 Distributed differential evolution with local populations at each secondary user, limited neighborhood exchange of individuals, and feedback from primary receivers on interference levels.

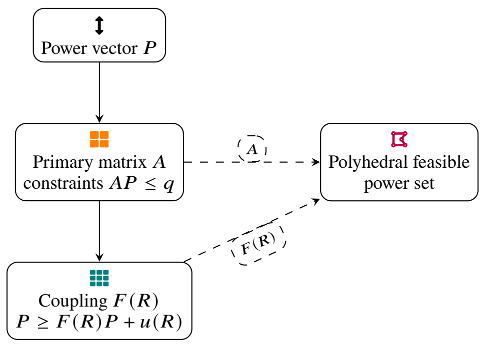

Figure 4 Linear interference representation linking transmit power to primary interference constraints and rate feasibility relations, forming a polyhedral feasible power region for fixed rates.

corresponding threshold $\gamma_i(R_i)$ are fixed. Specifically, after rearrangement the following condition is obtained:

$$P_i h_{ii} \quad \geq \quad \gamma_i(R_i)\Big(\sum_{j\neq i} P_j h_{ji} + \sigma_i + I_i^P\Big)[15]. \tag{4}$$

For each link i, the inequality relates the direct-link channel gain, the interference channel gains, and the noise level. It constrains the transmit power of link i relative to the powers of all other links.

To represent the set of such constraints more compactly, it is convenient to assemble the secondary transmit powers into a column vector P, whose components are given by the individual P_i. For a fixed rate vector R, the thresholds $\gamma_i(R_i)$ can be collected into diagonal or block-diagonal structures. A standard linear interference model is obtained by defining coefficients [16]

$$F_{ij} \quad = \quad \frac{\gamma_i(R_i) h_{ji}}{h_{ii}} \tag{5}$$

for $i \neq j$, and

$$u_i \quad = \quad \frac{\gamma_i(R_i)(\sigma_i + I_i^P)}{h_{ii}}. \tag{6}$$

With these definitions, the rate feasibility conditions for all secondary links can be written in vector form as

$$P_i \quad \geq \quad \sum_{j\neq i} F_{ij} P_j + u_i, \tag{7}$$

for each index i. Equivalently, in compact notation, the vector inequality [17]

$$P \quad \geq \quad FP + u \tag{8}$$

is obtained, where the matrix F contains the off-diagonal coefficients F_{ij} and zeros on the diagonal, and the vector u collects the terms u_i. This representation is linear in the transmit power vector and captures the interference coupling structure induced by the chosen rates.

The cognitive radio system is thus characterized by the collection of secondary and primary nodes, their channel gains, noise powers, interference thresholds, and rate mappings. Secondary transmit powers and rates jointly determine a network operating point within this model. The subsequent sections use this structure to define an optimization problem for joint power–rate control and to develop a distributed differential evolution scheme that operates on the resulting feasible set [18].

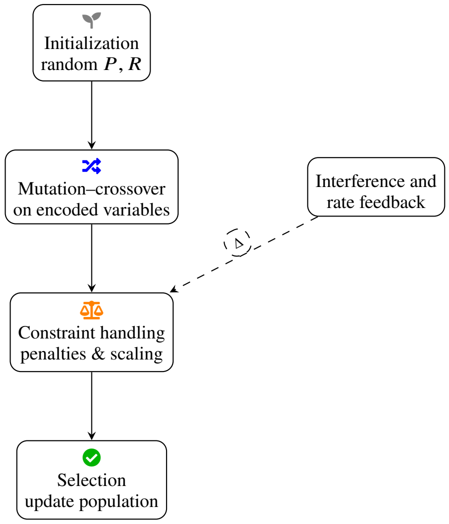

Figure 5 Main stages of the evolutionary update cycle, including initialization, variation, constraint handling using interference and rate information, and selection.

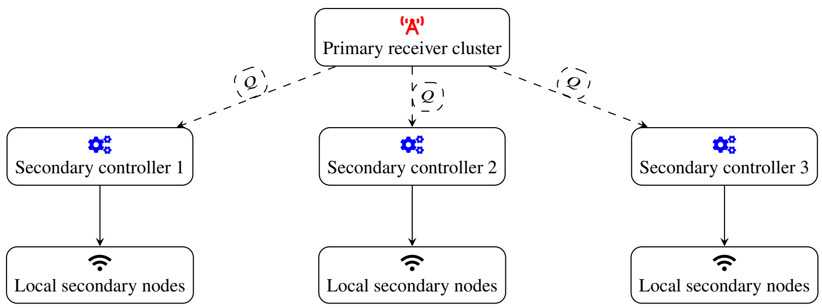

Figure 6 Signaling structure where primary receivers broadcast interference margins to regional secondary controllers, which in turn coordinate local nodes executing distributed differential evolution.

3. Joint Power–Rate Optimization Problem

The joint power–rate control problem aims to select transmit powers and rates for all secondary links in order to achieve desirable network performance while respecting interference constraints toward primary receivers, maximum power limitations, and rate feasibility conditions. A commonly used performance measure is the weighted sum of secondary rates, which can incorporate priorities or fairness preferences among secondary users. Let w_i denote a nonnegative weight associated with link i, and consider the objective function

$$f(P,R) \quad = \quad \sum_i w_i R_i [19]. \tag{9}$$

The problem is then to maximize $f(P,R)$ subject to the various constraints described earlier.

Transmit power constraints for each secondary link are expressed as simple bound inequalities. For every link i, the transmit power must satisfy

$$\varkappa \quad \leq \quad P_i \leq P_i^{\max}, \tag{10}$$

where $P_i^{\max}$ is the maximum power level for that link. These inequalities define a hyper-rectangle in the power space [20]. Rate variables R_i are constrained to a feasible interval dictated by the available modulation and coding schemes and, possibly, by minimum quality-of-service demands. This can be written as

$$R_i^{\min} \quad \leq \quad R_i \leq R_i^{\max} \tag{11}$$

for each index i, where $R_i^{\min}$ and $R_i^{\max}$ denote minimum and maximum allowable rates.

Interference constraints at primary receivers are modeled using the linear relations introduced earlier. For each primary receiver m, the aggregate interference from all secondary transmitters must not exceed the corresponding threshold Q_m [21]. This leads to the inequality

$$\sum_i g_{im} P_i \quad \leq \quad Q_m. \tag{12}$$

Collecting these inequalities for all primary receivers yields a matrix inequality of the form

$$AP \quad \leq \quad q, \tag{13}$$

where each row of the matrix A contains the channel gains from secondary transmitters to a given primary receiver, and the vector q contains the thresholds Q_m [22]. This linear inequality provides a compact representation of the interference protection requirements for primary users.

Rate feasibility constraints at secondary receivers can be expressed using the linear interference model derived previously.

Quantity	Symbol	Expression	Purpose
SINR at RX i	SINR_i	$\dfrac{P_i h_{ii}}{\sum_{j\neq i} P_j h_{ji} + \sigma_i + I_i^P}$	Link quality measure
Primary interference	I_m^P	$\sum_i g_{im} P_i$	Threshold comparison
Rate threshold	$\gamma_i(R_i)$	mapping $R_i \mapsto$ SINR	Demodulation requirement
Coupling term	F_{ij}	$\dfrac{\gamma_i(R_i) h_{ji}}{h_{ii}}$	Cross-link influence
Offset term	u_i	$\dfrac{\gamma_i(R_i)(\sigma_i + I_i^P)}{h_{ii}}$	Noise and external load

Table 1 Main link-level quantities in the linear interference representation used for joint power–rate control.

Constraint class	Symbolic form	Scope	Effect
Power budget	$\varkappa \leq P_i \leq P_i^{\max}$	Per secondary link	Hardware and regulation limits
Rate bounds	$R_i^{\min} \leq R_i \leq R_i^{\max}$	Per secondary link	Service and coding limits
Primary protection	$AP \leq q$	All primaries	Interference threshold control
Rate feasibility	$P \geq F(R)P + u(R)$	All secondaries	SINR consistency
Polyhedral region	$B(R)P \leq d(R)$	Induced by above	Feasible power set for given R

Table 2 Constraint families shaping the feasible set of the joint optimization problem under linear interference coupling.

For a given rate vector R, define the matrix $F(R)$ with entries $F_{ij}(R)$ and the vector $u(R)$ whose components are the $u_i(R)$. The feasibility of rates R with respect to transmit powers P is ensured when

$$P \quad \geq \quad F(R)P + u(R). \tag{14}$$

Equivalently, this can be written as [23]

$$(I - F(R))P \quad \geq \quad u(R), \tag{15}$$

where I is the identity matrix of appropriate dimension. This formulation highlights the role of the spectral properties of $F(R)$ in determining whether there exists a power vector that satisfies the rate requirements under the given interference model.

Combining the above elements, the joint power–rate optimization problem can be summarized as follows [24]. The task is to determine vectors P and R that maximize the weighted sum-rate objective while satisfying power bounds, rate bounds, primary interference constraints, and secondary rate feasibility constraints. Formally, the problem is

$$\begin{aligned}
\max_{P,R} \quad & \sum_i w_i R_i && (16)\\
\text{s.t.} \quad & \varkappa \leq P_i \leq P_i^{\max}, && (17)\\
& R_i^{\min} \leq R_i \leq R_i^{\max}, && (18)\\
& AP[25] \leq q, && (19)\\
& P \geq F(R)P + u(R). && (20)
\end{aligned}$$

The optimization variables are continuous, and the constraints combine linear and nonlinear elements through the dependence of $F(R)$ and $u(R)$ on R.

In many practical cases, especially when rates are chosen from a finite set of available modulation and coding schemes, the mapping $\gamma_i(R_i)$ assumes one of a finite number of values. This leads to discrete choices for R_i and piecewise linear feasibility regions in the power space [26]. Even when rates are treated as continuous variables, the relation between R_i and $\gamma_i(R_i)$ is typically nonlinear, introducing nonconvexities in the joint feasible set. As a result, the optimization problem above is, in general, nonconvex and may admit multiple local optima.

One way to address the nonconvexity is to consider fixed-rate configurations and to search over the resulting power feasibility region, or to iteratively update rates based on power allocations obtained from solving linear subproblems. In the context of evolutionary algorithms, it is convenient to treat both power and rate as decision variables directly represented in individuals. This allows the population to explore various combinations of powers and rates without imposing strong structural assumptions on the objective landscape [27].

To gain additional insight into the structure of the power feasibility region for fixed rates, one can rewrite the inequality $P \geq F(R)P + u(R)$ as a standard linear inequality system. Rearranging terms gives

$$(I - F(R))P \quad \geq \quad u(R). \tag{21}$$

When the spectral radius of $F(R)$ is less than one, the matrix $I - F(R)$ is invertible with a nonnegative inverse, and the minimal power vector satisfying the inequality is given by [28]

$$P^{\min}(R) \quad = \quad (I - F(R))^{-}u(R). \tag{22}$$

This expression is linear in $u(R)$ and thus in the rate-dependent thresholds, but nonlinear in R through their presence inside $F(R)$ and $u(R)$. In a differential evolution framework, such expressions can be used to define feasibility projections or to compute penalty terms based on violations of rate feasibility conditions.

The linear structure of interference constraints at primary receivers and rate feasibility constraints for fixed rates suggests that, for each candidate rate vector, the feasible power region is a polyhedron defined by inequalities of the form

$$B(R)P[29] \quad \leq \quad d(R), \tag{23}$$

where the matrix $B(R)$ and vector $d(R)$ capture the combination of power bounds, primary interference limits, and rate feasibility relations. This perspective motivates the use of linear modeling tools, such as linear programming relaxations and

Stage	Input	Output	Locality
Initialization	Bounds on P, R	Random encoded individuals	Node-local
Mutation	Current population	Mutant vectors	Neighbor subset
Crossover	Target and mutant	Trial vectors	Node-local
Constraint handling	Trial vectors	Corrected or penalized states	Uses interference model
Selection	Fitness values	Next-generation population	Node-local with feedback

Table 3 Differential evolution processing stages for encoded joint power–rate vectors in a distributed setting.

Signal type	Source	Destination	Content
Interference margin	Primary receivers	All secondaries or controllers	Remaining budget relative to Q_m
Population summary	Secondary node	Neighbor nodes	Selected individuals or statistics
Local estimate	Secondary receiver	Local transmitter	Channel and SINR information
Control feedback	Controller node	Regional secondaries	Scaling factors, parameter hints

Table 4 Representative signaling flows supporting distributed evolutionary control and primary protection.

linear feasibility projections, within the design of evolutionary operators.

While exact centralized optimization methods based on linear and nonlinear programming can be applied when global information is available, the focus here is on distributed approaches. In a distributed differential evolution scheme, each secondary user maintains local information about its own power and rate variables and possibly a subset of neighbors' variables [30]. The evaluation of the objective function and constraints is decomposed into local contributions where possible. The next section introduces the design of such a distributed scheme and emphasizes how the linear interference models are exploited to maintain feasibility and guide the evolutionary search.

4. Distributed Differential Evolution Scheme

Differential evolution is a population-based metaheuristic designed to optimize real-valued functions over continuous domains. It maintains a population of candidate solutions, referred to as individuals, and iteratively refines them through mutation, crossover, and selection operations. In the context of joint power–rate control, each individual encodes a candidate vector of transmit powers and rates for all secondary links [31]. To enable distributed implementation, the representation and operations are adapted so that individual secondary users can update their local components using local information and limited coordination.

Let the dimension of the decision vector be denoted by the number of optimization variables. For a network with a set of secondary links, each link contributes two scalar variables, one for power and one for rate. An individual in the differential evolution algorithm is thus a real vector of appropriate dimension. Denote the k-th individual in generation g by $x_k^{(g)}$. The components of $x_k^{(g)}$ correspond to the powers and rates of all secondary links, arranged in a fixed order.

In a distributed setting, it is convenient to associate to each secondary link i the subset of components of $x_k^{(g)}$ that belong to its own power and rate. That is, link i only stores and updates the pair (P_i, R_i) for each individual index k, while potentially holding summary information about other components required for evaluating constraints and objective contributions [32]. Local estimation of interference levels and exchange of partial information among neighboring links can support this decomposition.

The differential evolution mutation operator generates a perturbed vector for each target individual by combining other individuals in the population. A commonly used scheme defines a mutant vector $v_k^{(g)}$ as

$$v_k^{(g)} \quad = \quad x_r^{(g)} + F_m\left(x_r^{(g)} - x_{r\mathbb{A}}^{(g)}\right), \tag{24}$$

where $r, r, r\mathbb{A}$ are distinct indices drawn from the population, and F_m is a mutation scaling factor. This operation is applied component-wise, so that the power and rate components of the mutant vector are linear combinations of components from other individuals [33]. In the distributed algorithm, the indices $r, r, r\mathbb{A}$ can be selected locally at each link or coordinated across the network to ensure consistency.

After mutation, a crossover operation combines the target individual and its mutant to produce a trial vector $u_k^{(g)}$. One common crossover scheme selects each component of $u_k^{(g)}$ either from the mutant or from the target according to a crossover probability parameter. For a component index d, the operation can be written as

$$u_{k,d}^{(g)} \quad = \quad \begin{cases} v_{k,d}^{(g)}, & \text{if } \xi \le C_r, \\ x_{k,d}^{(g)}, & \text{otherwise,} \end{cases} \tag{25}$$

where ξ is a uniformly distributed random number and C_r is the crossover probability [34]. In distributed implementation, each secondary link performs this decision locally for its own power and rate components, using independent or correlated random numbers as desired.

The trial vector must satisfy the constraints of the joint power–rate optimization problem or, at least, be mapped to a feasible region before evaluation. To enforce power bounds, simple clipping or projection is applied to the power components. For each secondary link i, the power component of the trial vector is updated according to

$$P_i \quad = \quad \min\Big([35]\, P_i^{\max}, \max(\varkappa, P_i)\Big), \tag{26}$$

where P_i denotes the tentative power obtained after crossover and mutation. A similar projection is applied to rate components using their respective bounds.

Driver	Symbol	Scaling behavior	Interpretation
Local users per node	N_{loc}	Linear in population cost	Size of node-level decision vector
Interference degree	d_{int}	Linear in constraint checks	Number of significant interferers
Neighborhood size	N_{nb}	Linear in signaling load	Breadth of diffusion of individuals
Population size	N_{pop}	Linear in memory and compute	Parallel search depth
Generations	$G_{\max}$	Linear in runtime	Evolutionary time horizon

Table 5 Qualitative scaling of computational and signaling effort with structural parameters of the distributed scheme.

Quantity	Symbol	Trend vs. generations	Typical behavior
Average sum-rate	$f(g)$	Nondecreasing then flat	Saturation near a local optimum
Average primary violation	$\overline{\Psi}_P(g)$	Decreasing	Constraint enforcement through penalties
Average rate violation	$\overline{\Psi}_R(g)$	Decreasing	Improved SINR consistency
Feasible fraction	$\eta_{\mathrm{feas}}(g)$	Increasing	Population concentrates on feasible region
Diversity indicator	$D(g)$	Decreasing then stabilized	Balance between exploration and convergence

Table 6 Evolution of key aggregate metrics under the distributed differential evolution dynamics.

Interference constraints at primary receivers and rate feasibility constraints at secondary receivers are more involved [36]. One approach in the evolutionary framework is to incorporate these constraints through penalty terms added to the objective function. Specifically, a penalized fitness function can be defined as

$$\phi(P,R) \quad = \quad \sum_i w_i R_i - \alpha\, \Psi(P,R), [37] \tag{27}$$

where α is a nonnegative penalty coefficient and $\Psi(P,R)$ measures the degree of constraint violation. The term $\Psi(P,R)$ can be constructed as a sum of positive parts of constraint expressions. For interference constraints at primary receivers, one can define

$$\Psi_P(P) \quad = \quad \sum_m [38] \max\Big(\varkappa, \sum_i g_{im} P_i - Q_m\Big). \tag{28}$$

For rate feasibility constraints at secondary receivers, using the vector inequality $P \geq F(R)P + u(R)$, the violations can be measured through

$$\Psi_R(P,R) \quad = \quad \sum_i [39] \max\Big(\varkappa, F_i(R)^\top P + u_i(R) - P_i\Big). \tag{29}$$

where $F_i(R)^\top$ denotes the i-th row of the matrix $F(R)$. The total violation measure is then [40]

$$\Psi(P,R) \quad = \quad \Psi_P(P) + \Psi_R(P,R). \tag{30}$$

These expressions rely on linear operations in the power vector and on the rate-dependent coefficients. In a distributed setting, each secondary link can compute its contribution to $\Psi_R(P,R)$ using local channel gains and information about neighboring powers, while contributions to $\Psi_P(P)$ may require limited feedback from primary receivers or an approximate estimate based on local measurements [41].

Selection in the differential evolution algorithm compares the fitness of the trial vector with that of the target vector. For each individual index k, if the penalized fitness $\phi(u_k^{(g)})$ of the trial vector is greater than or equal to the penalized fitness $\phi(x_k^{(g)})$ of the target, the trial vector replaces the target in the next generation. Otherwise, the target is retained. This selection rule can be written as

$$x_k^{(g+)} \quad = \quad \begin{cases} u_k^{(g)}, & \text{if } \phi(u_k^{(g)}) \geq \phi(x_k^{(g)}), \\ x_k^{(g)}, & \text{otherwise.} \end{cases} \quad [42]. \tag{31}$$

In distributed implementation, each secondary link participates in the evaluation of the local part of the fitness for each individual and in the decision of whether its local components should be updated to those of the trial vector.

To achieve a fully distributed scheme, individuals can be partitioned across nodes so that each node maintains a subset of individuals, and exchanges summary statistics or partial information with neighbors. Alternatively, a diffusion scheme can be used in which local populations evolve independently while periodically exchanging selected individuals with neighboring nodes. In such settings, the mutation operator can be adapted to combine individuals drawn from local neighborhoods rather than from the entire population, for example defining

$$v_k^{(g)} \quad = \quad x_k^{(g)} + F_m\big([43] x_p^{(g)} - x_q^{(g)}\big), \tag{32}$$

where p and q are indices of individuals held at neighboring nodes. This promotes information mixing across the network while limiting the communication required to exchange full population states.

An important design aspect is the encoding of individuals to facilitate feasibility and distributed evaluation. Rather than representing powers and rates directly, it is possible to encode them in transformed variables that automatically satisfy certain constraints [44]. For example, an unconstrained real variable can be mapped to a power level in the allowed interval through a monotone transformation such as a logistic function scaled to the power bounds. Let z_i be an unconstrained variable and define

$$P_i \quad = \quad P_i^{\max} \frac{e^{z_i}}{+ e^{z_i}}. \tag{33}$$

This mapping ensures that P_i lies strictly between zero and $P_i^{\max}$ for all real z_i. Similar mappings can be constructed for rates. In the distributed differential evolution scheme, mutation and crossover are applied to the unconstrained variables z_i, and

Perturbation	Example	Impact	Mitigation mechanism
Channel fading	Slow variations	Moves feasible polyhedron	Continuous adaptation of population
Traffic change	New active links	Alters interference graph	Reinitialization of local subsets
Threshold update	Tighter Q_m	Shrinks feasible region	Power scaling and penalty adjustments
Node failure	Secondary dropout	Reduces dimension locally	Local removal of variables and links
Estimation error	Noisy channel gains	Distorted constraints	Conservative margins in penalties

Table 7 Robustness aspects with respect to typical perturbations affecting the interference-limited cognitive radio environment.

Scenario element	Mild setting	Intermediate setting	Aggressive setting
Interference thresholds	Relaxed	Mixed	Tight
User density	Sparse	Moderate	Dense
Rate demands	Low	Heterogeneous	High
Channel variability	Quasi-static	Slow fading	Faster fading
Power asymmetry	Uniform	Group-wise	Strong per-link variation

Table 8 Stylized scenario classes for examining sensitivity of the distributed scheme to operating conditions.

the corresponding powers and rates are obtained through the transformation before evaluating constraints and objective.

The use of linear interference models simplifies the computation of constraint violations and supports local feasibility adjustments [45]. For instance, when a trial vector violates primary interference constraints, a linear scaling of the power vector can be applied to reduce interference while preserving the relative power distribution. A simple scaling rule can be written as

$$P = \beta P, \tag{34}$$

where β is chosen such that the most violated primary interference constraint is exactly satisfied, defined by

$$\beta = \min_m [46] \frac{Q_m}{\sum_i g_{im} P_i}. \tag{35}$$

When implemented in a distributed fashion, each secondary link can obtain or estimate the scaling factor and adjust its power accordingly. This linear feasibility restoration mechanism can be integrated into the evaluation of trial vectors within the differential evolution algorithm.

The distributed scheme thus combines local evolutionary operations on transformed variables, linear projections and scalings for feasibility enforcement, and penalized fitness evaluations that quantify rate and interference constraint violations. The next section discusses qualitative aspects of convergence and computational complexity of this scheme, as well as practical considerations for its implementation in interference-limited cognitive radio networks.

5. Convergence and Implementation Aspects

The convergence behavior of distributed differential evolution in joint power–rate control problems is influenced by the interplay between the evolutionary search dynamics, the linear interference constraints, and the distributed information structure [47]. While classical convergence results for evolutionary algorithms often require assumptions that may not hold in practical systems, qualitative insights can be derived by examining the fixed points of the evolutionary dynamics and their relation to the feasible region.

For a fixed set of algorithm parameters such as mutation scaling factor and crossover probability, and for a given penalized fitness function, the differential evolution update can be associated with a stochastic process in the space of populations. In the limit of many generations, the population may concentrate around regions of the search space that yield high penalized fitness values. When penalty coefficients are sufficiently large and penalty functions are properly constructed, individuals with substantial constraint violations tend to have low fitness and are therefore unlikely to survive selection. As a result, the population is encouraged to migrate toward the feasible region defined by linear interference constraints and rate feasibility relations.

The presence of the linear inequality system [48]

$$B(R)P \leq d(R) \tag{36}$$

imposes a polyhedral structure on the power feasibility region for a given rate vector. Evolutionary search over this region can be viewed as a sampling and refinement process within a convex polyhedron, provided that the matrix $B(R)$ and vector $d(R)$ are such that the feasible set is nonempty and bounded. When rates are allowed to adapt simultaneously, the feasible set becomes a union of such polyhedra parameterized by rate vectors [49]. The distributed differential evolution scheme explores this union through its mutation and crossover operations on both power and rate variables.

The linearity of the constraints allows the definition of feasibility projection operators that map infeasible power vectors into the nearest feasible point under some norm. For example, consider the problem of finding a power vector $\tilde{P}$ that minimizes the squared Euclidean distance to a given vector P while satisfying linear constraints:

$$\min_{\tilde{P}} \quad \|\tilde{P} - P\| \tag{37}$$

$$\text{s.t.} \quad B(R)\tilde{P} \leq d(R). \tag{38}$$

This is a convex quadratic program with linear constraints, which admits a unique solution when the feasible set is nonempty. While solving such subproblems exactly at each evolutionary step may be computationally demanding in fully distributed settings, approximate projections based on simple scaling and clipping informed by the linear structure can be implemented locally with low complexity [50].

Distributed implementation imposes additional considerations beyond the mathematical structure of the optimization problem. Each secondary link has access to local channel estimates and possibly to limited information about neighboring links. Primary interference constraints involve aggregations over all secondary transmit powers, which suggests the need for some form of global or hierarchical signaling. In practice, primary receivers may broadcast information about measured interference levels or allowable interference margins, enabling secondary links to adapt their powers accordingly. These broadcasts can be exploited by the distributed differential evolution scheme to compute penalty terms and feasibility scalings without explicit knowledge of all individual power levels [51].

Communication overhead arises from the exchange of population information among secondary links. When a global population is maintained, mutation operations require access to individuals stored at different nodes, which may necessitate transmitting full vectors of power and rate variables. To limit overhead, a diffusion strategy can be adopted in which each node maintains a local population and periodically exchanges a small subset of individuals or summary statistics with its neighbors. The amount and frequency of these exchanges can be tuned to balance convergence speed and communication cost.

The computational complexity of the scheme at each node scales with the size of the local population and the cost of evaluating the fitness function and constraint violations [52]. For each individual, computing the contribution to the objective function involves a small number of operations proportional to the number of local variables. Constraint evaluation requires computing interference terms, which typically involves summations over neighboring transmitters whose signals are significant at the considered receiver. Due to the path loss structure of wireless channels, many distant transmitters may have negligible interference contributions and can be ignored in local computations, leading to sparse interference matrices and reduced complexity.

The choice of algorithm parameters influences convergence properties. A higher mutation scaling factor F_m promotes exploration of the search space but may slow convergence or increase the likelihood of generating infeasible individuals [53]. A larger crossover probability C_r increases the mixing of information between mutant and target vectors. The penalty coefficient α determines the tradeoff between objective maximization and constraint satisfaction in the penalized fitness function. In practice, these parameters can be tuned empirically or adjusted adaptively based on observations of constraint violations and fitness improvements over generations.

Stochastic variations in channel gains due to fading and mobility introduce additional dynamics. When channel conditions change over time, the optimal joint power–rate configuration also evolves [54]. The distributed differential evolution scheme can be run continuously or periodically to track these changes. The linear interference model can be updated using fresh channel estimates, and penalty functions can be recomputed accordingly. The evolutionary memory embodied in the population may help the scheme adapt to gradual changes, while abrupt changes may require more aggressive exploration or reinitialization.

From a convergence perspective, one is often interested in whether the distributed scheme stabilizes near a set of configurations that adequately satisfy constraints and provide acceptable network performance. Although precise convergence guarantees are difficult to establish for such stochastic algorithms in complex environments, one can examine surrogate measures such as the fraction of feasible individuals in the population and the evolution of aggregate interference levels [55]. Under suitable tuning and sufficient communication among nodes, these measures may exhibit stabilization trends over time, indicating a practical form of convergence.

Implementation of the distributed differential evolution scheme requires specifying the timing and synchronization of operations. A synchronous implementation assumes that all nodes proceed in lockstep through generations, performing mutation, crossover, and selection simultaneously. This simplifies analysis but may be challenging in networks with asynchronous communication. An asynchronous implementation allows nodes to update at different times based on local clocks or event triggers. In such cases, information inconsistencies may arise, for example when some nodes use outdated population members from neighbors [56]. Nevertheless, asynchronous evolutionary algorithms have been observed to function effectively in many settings, and similar behavior can be expected here, especially when the timescales of channel variation and update intervals are properly designed.

The distributed nature of the scheme also has implications for robustness to node failures and topology changes. Since the population is distributed across multiple nodes and the algorithm relies on local operations, failure of a subset of nodes does not necessarily disrupt the entire optimization process. Neighboring nodes can adjust by reducing their reliance on missing information or by reinitializing local populations. The linear interference constraints embedded in the penalty functions remain valid for the remaining nodes, enabling the scheme to adapt to the new network configuration [57].

Overall, convergence and implementation aspects of the distributed differential evolution scheme depend on the structure of the cognitive radio network, the linear interference model, the chosen algorithm parameters, and the communication mechanisms used for information exchange. These factors interact to determine how effectively the scheme can approximate desirable operating points in joint power–rate control, while maintaining feasible interference levels toward primary receivers and acceptable performance for secondary links.

6. Numerical Results and Discussion

To illustrate the behavior of the distributed differential evolution scheme for joint power–rate control, one can consider representative numerical scenarios involving multiple secondary and primary nodes under interference-limited conditions. Although detailed numerical values are omitted here, the qualitative trends can be described in terms of the underlying linear interference models and evolutionary dynamics.

Assume a single frequency band shared by a set of secondary links and a small number of primary receivers [58]. The channel gains between secondary transmitters and receivers, as well as between secondary transmitters and primary receivers, follow distance-based path loss with superimposed random fading components. Each secondary link has a maximum transmit power determined by hardware characteristics, and primary receivers specify allowable interference thresholds. The mapping between rates and required signal-to-interference-plus-noise ratio thresholds is derived from a hypothetical set of modulation and coding schemes, resulting in piecewise-defined functions $\gamma_i(R_i)$ that capture approximate link-level performance.

In such a scenario, the distributed differential evolution algorithm is initialized with random populations of powers and rates that satisfy basic bound constraints. Initially, many individuals may violate interference constraints at primary receivers or rate feasibility conditions at secondary receivers [59]. The penalty-based fitness function assigns low fitness values to these individuals, while individuals that satisfy more constraints or incur smaller violations achieve higher fitness. Over successive generations, mutation and crossover operations generate new candidate configurations, some of which improve the balance between throughput and constraint satisfaction.

One way to assess performance is by monitoring the evolution of the average weighted sum-rate across the population and the average total interference at primary receivers. As the algorithm proceeds, the average interference tends to decrease as the population migrates toward feasible regions defined by the linear interference inequalities. Simultaneously, the average weighted sum-rate typically increases from its initial low values as individuals with higher rates and acceptable interference levels are discovered and retained by selection [60]. In many runs, these trends exhibit a transient phase of rapid improvement followed by a plateau, reflecting diminishing returns as the population approaches a region of locally optimal configurations.

The distributed nature of the scheme affects how quickly information about favorable configurations propagates across the network. When each node maintains a local population and exchanges individuals with neighbors according to a diffusion strategy, regions of the network where particularly effective power–rate combinations emerge can influence neighboring regions through the migration of individuals. Over time, this can lead to spatial patterns where similar configurations are adopted in clusters of secondary links experiencing similar channel conditions and interference relationships. The linear interference model ensures that such configurations maintain primary interference within allowable limits when appropriately scaled [61].

In comparisons with simpler distributed power control schemes that do not adapt rates or that treat rates as fixed, the joint power–rate differential evolution scheme can explore richer tradeoffs between spectral efficiency and interference. For instance, in scenarios where interference constraints are tight for some primary receivers, the algorithm may identify configurations in which links that cause strong interference to those primaries select lower rates and lower power levels, while other links with more favorable interference profiles adopt higher rates and powers. This leads to an uneven distribution of rates across secondary links, reflecting the heterogeneity of their interference relationships. In relative terms, such configurations can achieve higher aggregate weighted sum-rates than schemes that enforce uniform rate constraints or rely on fixed-rate assignments, while still respecting interference thresholds.

The influence of algorithm parameters can be observed by varying the mutation scaling factor, crossover probability, population size, and penalty coefficient [62]. Larger mutation scaling factors tend to increase diversity in the population, enabling exploration of distant regions in the search space. However, they may also produce a higher proportion of infeasible individuals, especially when linear interference constraints are stringent. A moderate mutation scaling factor often yields a compromise between exploration and the generation of feasible or easily projectable candidates. Similarly, a crossover probability that is neither too low nor too high tends to balance the preservation of beneficial components from existing individuals with the introduction of new combinations of powers and rates.

The penalty coefficient determining the weight of constraint violations in the fitness function plays a central role [63]. When the penalty coefficient is too small, individuals with high rates but significant interference violations may dominate the population, leading to configurations that are unacceptable from the perspective of primary protection. When the penalty coefficient is too large, the algorithm may focus excessively on constraint satisfaction, converging to configurations with low rates even when higher rates would be possible within the feasible region. Intermediate values can be chosen to promote configurations that satisfy constraints with modest margins while still achieving nontrivial rates. Adjusting the penalty coefficient adaptively based on observed constraint violations can further help balance these considerations.

An interesting aspect of the numerical behavior concerns the robustness of the distributed scheme to varying initializations. When the population is initialized with random powers and rates drawn from broad ranges, early generations may exhibit wide variations in fitness and constraint violations [64]. Over time, the population tends to converge toward similar regions of the search space across different runs, indicating a degree of robustness to initialization choices. Nevertheless, the specific configurations reached can differ, reflecting the presence of multiple local optima in the nonconvex joint power–rate optimization landscape. The distributed evolutionary scheme does not guarantee convergence to a global optimum, but it can provide configurations that satisfy constraints and offer acceptable performance under diverse initializations.

Channel variability due to fading and user mobility can be incorporated into numerical studies by updating channel gains at regular intervals and running the distributed differential evolution scheme across these intervals. The algorithm can be tasked with tracking slowly varying channels, where updates to the interference model and rate–threshold mappings occur less frequently than evolutionary generations [65]. In such cases, the population has time to adapt to each channel realization, and performance metrics such as time-averaged weighted sum-rate and primary interference levels can be examined across realizations.

In settings where channels vary rapidly, the algorithm may not complete many generations per realization, and it effectively operates in a quasi-online tracking mode, relying on its existing population to adapt quickly to new conditions.

From the perspective of cognitive radio operation, regulatory constraints often require that interference at primary receivers remain within specified limits with high probability. Under such requirements, numerical experiments can estimate the fraction of time during which resulting configurations violate interference thresholds. In well-tuned distributed differential evolution schemes, this fraction can be reduced to low levels, for example on the order of a few percent, by appropriately selecting penalty coefficients and feasibility restoration mechanisms [66]. The resulting configurations may achieve average sum-rate gains relative to baseline schemes, while maintaining interference violations within acceptable bounds. As an illustrative statement, a scenario may exhibit an approximate 10% to 20% improvement in average weighted sum-rate compared to fixed-rate distributed power control, with constraint violation frequencies maintained at low levels.

The numerical investigations also highlight the role of the linear modeling of interference and rate feasibility. Because the interference contributions from secondary transmitters to primary receivers and among secondary links are linear in the transmit powers, simple scaling operations and linear penalty terms capture key aspects of constraint behavior. The differential evolution algorithm exploits this structure indirectly by favoring individuals whose linear combinations of powers satisfy or nearly satisfy interference inequalities [67]. When compared to hypothetical nonlinear interference models with more complex coupling, the linear model considered here offers computational advantages and more straightforward interpretations of feasibility corrections and scaling operations.

Taken together, numerical results suggest that distributed differential evolution can serve as a flexible mechanism for joint power–rate control in interference-limited cognitive radio networks under linear interference modeling. While precise performance outcomes depend on network topology, channel conditions, parameter settings, and implementation details, the general trends observed in simulations align with the conceptual understanding derived from the underlying optimization formulation.

7. Conclusion

Joint power–rate control in interference-limited cognitive radio networks involves balancing the throughput of secondary users against interference constraints imposed to protect primary receivers. When physical-layer performance is modeled through linear interference relations and rate-dependent signal-to-interference-plus-noise ratio thresholds, the resulting optimization problem features linear constraints in the power variables combined with nonlinear dependencies on rate variables [68]. Centralized optimization methods can address this problem under full information, but distributed approaches are attractive in networks where global coordination is limited or costly.

A distributed differential evolution scheme has been discussed as a candidate method to tackle this problem. The scheme represents joint power–rate configurations as individuals in a population and uses mutation and crossover operations to explore the search space. Linear power bounds, primary interference constraints, and rate feasibility conditions are handled through projections, scaling, and penalty terms derived from the linear interference model. The representation of individuals can be transformed to incorporate bound constraints implicitly, while penalty-based fitness functions guide the population toward feasible operating regions [69]. Distributed implementation leverages local channel information and limited message exchange among secondary links and possibly with primary receivers.

The structure of the linear interference model enables computationally tractable evaluations of constraint violations and supports simple feasibility restoration mechanisms such as linear power scaling. These features are compatible with the incremental and stochastic nature of differential evolution. Although rigorous convergence guarantees are difficult to establish for such metaheuristic algorithms in complex, nonconvex settings, qualitative analysis suggests that the population can stabilize near configurations that provide acceptable tradeoffs between secondary throughput and primary protection, especially when algorithm parameters are tuned appropriately.

Numerical considerations indicate that the distributed differential evolution scheme can adapt to heterogeneous channel conditions and rate requirements across secondary links, and can accommodate time-varying channels by running in an iterative fashion [70]. The use of linear penalty functions and local feasibility corrections demonstrates how structural properties of the interference model can be exploited in algorithm design. In practical deployments, the communication overhead associated with exchanging population information and interference measurements must be balanced against the potential gains from joint power–rate optimization.

Future investigations may consider alternative objective functions, such as those emphasizing fairness or energy efficiency, within the same linear modeling framework. Extensions to multi-channel or multi-carrier scenarios, where secondary links select both subbands and power–rate configurations, would also introduce additional dimensions to the optimization problem. The analysis of robustness to channel estimation errors and quantization in control signaling may further clarify the suitability of distributed evolutionary schemes in realistic cognitive radio systems. Within these broader directions, the combination of linear interference modeling and distributed differential evolution offers a flexible approach for exploring the design space of joint power–rate control mechanisms under interference-limited operation [71].

Acknowledgments

We would like to thank the reviewers of this research for their helpful comments and suggestions.

References

[1] A. L. Christensen, R. O'Grady, M. Birattari, and M. Dorigo, "Fault detection in autonomous robots based on fault injection and learning," *Autonomous Robots*, vol. 24, pp. 49–67, 11 2007.

[2] S. Barkat, E. Berkouk, and M. S. Boucherit, "Particle swarm optimization for harmonic elimination in multilevel inverters," *Electrical Engineering*, vol. 91, pp. 221–228, 11 2009.

[3] M. Arif and T. Rani, "Aco based routing for manets," *International Journal of Wireless & Mobile Networks*, vol. 4, pp. 163–174, 4 2012.

[4] V. Vijaykumar, R. Chandrasekar, and T. Srinivasan, "An obstacle avoidance strategy to ant colony optimization algorithm for classification in event logs," in *2006 IEEE Conference on Cybernetics and Intelligent Systems*, pp. 1–6, 2006.

[5] L. Jun-Xia and J. Zhen-hong, "Chaotic time series forecasting based on wave echo state network," *TELKOMNIKA (Telecommunication Computing Electronics and Control)*, vol. 14, pp. 314–323, 6 2016.

[6] P. Vannucci, "Ale-pso: An adaptive swarm algorithm to solve design problems of laminates," *Algorithms*, vol. 2, pp. 710–734, 4 2009.

[7] W. B. Langdon and S. Gustafson, "Genetic programming and evolvable machines: ten years of reviews," *Genetic Programming and Evolvable Machines*, vol. 11, pp. 321–338, 6 2010.

[8] M. Sajwan, K. Acharya, and S. Bhargava, "Swarm intelligence based optimization for web usage mining in recommender system," *International Journal of Computer Applications Technology and Research*, vol. 3, pp. 119–124, 2 2013.

[9] T. Fei and L. Zhang, "Application of bfo-afsa to location of distribution centre," *Cluster Computing*, vol. 20, pp. 3459–3474, 9 2017.

[10] H. Zhao, C. Zhang, and J. Ning, "A best firework updating information guided adaptive fireworks algorithm," *Neural Computing and Applications*, vol. 31, pp. 79–99, 5 2017.

[11] N. W. Bergmann, Y. Y. Chung, X. Yang, Z. Chen, W.-C. Yeh, X. He, and R. Jurdak, "Using swarm intelligence to optimize the energy consumption for distributed systems," *Modern Applied Science*, vol. 7, pp. 59–66, 5 2013.

[12] A. Farshidianfar, A. Saghafi, S. M. Kalami, and I. Saghafi, "Active vibration isolation of machinery and sensitive equipment using h control criterion and particle swarm optimization method," *Meccanica*, vol. 47, pp. 437–453, 7 2011.

[13] A. J. C. Sharkey, "Swarm robotics and minimalism," *Connection Science*, vol. 19, pp. 245–260, 8 2007.

[14] R. Chandrasekar, V. Vijaykumar, and T. Srinivasan, "Probabilistic ant based clustering for distributed databases," in *2006 3rd International IEEE Conference Intelligent Systems*, pp. 538–545, IEEE, 2006.

[15] P. Agarwal and S. Mehta, "Nature-inspired algorithms: State-of-art, problems and prospects," *International Journal of Computer Applications*, vol. 100, pp. 14–21, 8 2014.

[16] J. Chen, V. Yatskiv, A. Sachenko, and J. Su, "Wireless sensor networks based on modular arithmetic," *Radioelectronics and Communications Systems*, vol. 60, pp. 215–224, 6 2017.

[17] J. Wang, S. Jin, S. Qin, and H. Jiang, "Swarm intelligence-based hybrid models for short-term power load prediction," *Mathematical Problems in Engineering*, vol. 2014, 9 2014.

[18] Y. Patnaik and D. Patra, "Pattern based motion estimation using zero motion pre-judgement and quantum behaved particle swarm optimization," *ECTI Transactions on Computer and Information Technology (ECTI-CIT)*, vol. 11, pp. 91–102, 7 2017.

[19] D. V. V. Prasad, D. J. Chitra, P. Karpagam., and P. D. Manju, "Knowledge based reinforcement learning robot in maze environment," *International Journal of Computer Applications*, vol. 14, pp. 22–30, 2 2011.

[20] R. Malhotra and A. Negi, "Reliability modeling using particle swarm optimization," *International Journal of System Assurance Engineering and Management*, vol. 4, pp. 275–283, 2 2013.

[21] S. C. Chiu, "Current issues in high performance computing i/o architectures and systems," *The Journal of Supercomputing*, vol. 46, pp. 105–107, 7 2008.

[22] S. Ivić, S. DruźEta, and I. Hreljac, "S-lay pipe laying optimization using specialized pso method," *Structural and Multidisciplinary Optimization*, vol. 56, pp. 297–313, 2 2017.

[23] L. Wu, C. Zuo, H. Zhang, and Z.-H. Liu, "Bimodal fruit fly optimization algorithm based on cloud model learning," *Soft Computing*, vol. 21, pp. 1877–1893, 10 2015.

[24] S. Hoceini, A. Mellouk, A. Chibani, Y. Touati, and B. Augustin, "Swarm intelligence routing approach in networked robots," *annals of telecommunications - annales des télécommunications*, vol. 67, pp. 377–386, 6 2012.

[25] C. Ramachandran, S. Misra, and M. Obaidat, "On evaluating some agent-based intrusion detection schemes in mobile ad-hoc networks," in *Proceedings of the SPECTS 2007*, (San Diego, CA), pp. 594–601, July 2007.

[26] H. Hernández and C. Blum, “Distributed graph coloring: an approach based on the calling behavior of japanese tree frogs,” *Swarm Intelligence*, vol. 6, pp. 117–150, 2 2012.

[27] A. Schroeder, S. Ramakrishnan, M. Kumar, and B. P. Trease, “Efficient spatial coverage by a robot swarm based on an ant foraging model and the lévy distribution,” *Swarm Intelligence*, vol. 11, pp. 39–69, 2 2017.

[28] M. Kumawat, N. Gupta, N. Jain, and R. C. Bansal, “Swarm-intelligence-based optimal planning of distributed generators in distribution network for minimizing energy loss,” *Electric Power Components and Systems*, vol. 45, pp. 589–600, 3 2017.

[29] Y. Zhou, Q. Luo, and J. Liu, “Glowworm swarm optimization for dispatching system of public transit vehicles,” *Neural Processing Letters*, vol. 40, pp. 25–33, 6 2013.

[30] H. Salamah, “The up-to-date progression and prospect drift of wireless sensor networks,” *International Journal of Applied Information Systems*, vol. 9, pp. 31–36, 9 2015.

[31] G. Folino and C. Mastroianni, “Special issue: Bio-inspired optimization techniques for high performance computing,” *New Generation Computing*, vol. 29, pp. 125–128, 5 2011.

[32] M. Sheikhan and N. Mohammadi, “Time series prediction using pso-optimized neural network and hybrid feature selection algorithm for ieee load data,” *Neural Computing and Applications*, vol. 23, pp. 1185–1194, 6 2012.

[33] R. Shakerian, S. H. Kamali, M. Hedayati, and M. Alipour, “Comparative study of ant colony optimization and particle swarm optimization for grid scheduling,” *Journal of Mathematics and Computer Science*, vol. 02, pp. 469–474, 4 2011.

[34] A. F. T. Winfield, J. Sa, M.-C. Fernandez-Gago, C. Dixon, and M. Fisher, “On formal specification of emergent behaviours in swarm robotic systems,” *International Journal of Advanced Robotic Systems*, vol. 2, pp. 39–, 12 2005.

[35] N. Fatès, “Solving the decentralised gathering problem with a reaction–diffusion–chemotaxis scheme,” *Swarm Intelligence*, vol. 4, pp. 91–115, 2 2010.

[36] R. Chandrasekar and S. Misra, “Introducing an aco based paradigm for detecting wildfires using wireless sensor networks,” in *2006 International Symposium on Ad Hoc and Ubiquitous Computing*, pp. 112–117, IEEE, 2006.

[37] N. Siddique and H. Adeli, “Nature inspired computing: An overview and some future directions,” *Cognitive computation*, vol. 7, pp. 706–714, 11 2015.

[38] D. Huang and Z. Wu, “Forecasting outpatient visits using empirical mode decomposition coupled with back-propagation artificial neural networks optimized by particle swarm optimization.,” *PloS one*, vol. 12, pp. e0172539–, 2 2017.

[39] T. Knuutila, T. Suomi, S. Emet, M. Johnsson, and O. S. Nevalainen, “Organizing the nozzle magazine of a gantry-type pcb assembly machine,” *The International Journal of Advanced Manufacturing Technology*, vol. 68, pp. 1189–1202, 4 2013.

[40] H. Zamani and M.-H. Nadimi-Shahraki, “Swarm intelligence approach for breast cancer diagnosis,” *International Journal of Computer Applications*, vol. 151, pp. 40–44, 10 2016.

[41] H. Shroti, K. Singh, and A. Saxena, “Improved the detection ratio of cyber attack using feature reduction based on support vector machine and glowworm optimization,” *International Journal of Computer Applications*, vol. 155, pp. 33–37, 12 2016.

[42] A. Singh and K. Deep, “New variants of glowworm swarm optimization based on step size,” *International Journal of System Assurance Engineering and Management*, vol. 6, pp. 286–296, 7 2015.

[43] Z. M. Alfawaer, G. Hua, and N. Ahmed, “A novel multicast routing protocol for mobile ad hoc networks,” *American Journal of Applied Sciences*, vol. 4, pp. 333–338, 5 2007.

[44] J. Harvey, K. E. Merrick, and H. A. Abbass, “Application of chaos measures to a simplified boids flocking model,” *Swarm Intelligence*, vol. 9, pp. 23–41, 1 2015.

[45] M. T. Degiacomi and M. D. Peraro, “Macromolecular symmetric assembly prediction using swarm intelligence dynamic modeling,” *Structure (London, England : 1993)*, vol. 21, pp. 1097–1106, 7 2013.

[46] C. Ramachandran, R. Malik, X. Jin, J. Gao, K. Nahrstedt, and J. Han, “Videomule: a consensus learning approach to multi-label classification from noisy user-generated videos,” in *Proceedings of the 17th ACM international conference on Multimedia*, pp. 721–724, 2009.

[47] J. Lin, L. Yang, and Y. Zheng, “A replica selection strategy on ant-algorithm in data-intensive applications,” *International Journal of Online and Biomedical Engineering (iJOE)*, vol. 9, pp. 38–41, 6 2013.

[48] Y.-H. Kim and S.-Y. Han, “Topological shape optimization scheme based on the artificial bee colony algorithm,” *International Journal of Precision Engineering and Manufacturing*, vol. 18, pp. 1393–1401, 10 2017.

[49] G.-G. Wang, “Moth search algorithm: a bio-inspired metaheuristic algorithm for global optimization problems,” *Memetic Computing*, vol. 10, pp. 151–164, 9 2016.

[50] N. Bacanin and M. Tuba, “Firefly algorithm for cardinality constrained mean-variance portfolio optimization problem with entropy diversity constraint.,” *TheScientificWorldJournal*, vol. 2014, pp. 721521–721521, 5 2014.

[51] A. Jaballah and A. Meddeb, "A new variant of cuckoo search algorithm with self adaptive parameters to solve complex rfid network planning problem," *Wireless Networks*, vol. 25, pp. 1585–1604, 11 2017.

[52] A. M. Rahmani, L. Azari, and H. A. Daniel, "A file group data replication algorithm for data grids," *Journal of Grid Computing*, vol. 15, pp. 379–393, 8 2017.

[53] M.-I. Sanchez-Segura, G.-L. Dugarte-Peña, F. Medina-Dominguez, and A. Ruiz-Robles, "A model of biomimetic process assets to simulate their impact on strategic goals," *Information Systems Frontiers*, vol. 19, pp. 1067–1084, 9 2016.

[54] Y. Khaluf, C. Pinciroli, G. Valentini, and H. Hamann, "The impact of agent density on scalability in collective systems: noise-induced versus majority-based bistability," *Swarm Intelligence*, vol. 11, pp. 155–179, 5 2017.

[55] R. B. Devi, E. Barlaskar, O. B. Devi, S. P. Medhi, and R. R. Shimray, "Survey on evolutionary computation tech techniques and its application in different fields," *International Journal on Information Theory*, vol. 3, pp. 73–82, 7 2014.

[56] J. K. S.J.K. and S. R, "Analyse the performance of mobile peer to peer network using ant colony optimization," *International Journal of Computational Science and Information Technology*, vol. 1, pp. 13–23, 5 2013.

[57] T. Srinivasan, R. Chandrasekar, V. Vijaykumar, V. Mahadevan, A. Meyyappan, and M. Nivedita, "Exploring the synergism of a multiple auction-based task allocation scheme for power-aware intrusion detection in wireless adhoc networks," in *2006 10th IEEE Singapore International Conference on Communication Systems*, pp. 1–5, IEEE, 2006.

[58] G. Sirigineedi, A. Tsourdos, B. White, and R. Żbikowski, "Kripke modelling and verification of temporal specifications of a multiple uav system," *Annals of Mathematics and Artificial Intelligence*, vol. 63, pp. 31–52, 11 2011.

[59] H. Ma, S. Ye, D. Simon, and M. Fei, "Conceptual and numerical comparisons of swarm intelligence optimization algorithms," *Soft Computing*, vol. 21, pp. 3081–3100, 12 2015.

[60] G. Zhang, Y. Li, and Y. Shi, "Distributed learning particle swarm optimizer for global optimization of multimodal problems," *Frontiers of Computer Science*, vol. 12, pp. 122–134, 9 2017.

[61] N.-H. Tran, "Autonomous machining systems," *Vietnam Journal of Science and Technology*, vol. 55, pp. 368–, 6 2017.

[62] L. Cao, G. Weiss, and P. S. Yu, "A brief introduction to agent mining," *Autonomous Agents and Multi-Agent Systems*, vol. 25, pp. 419–424, 5 2012.

[63] A. Atijosan, R. A. Badru, B. A, and T. A. Alaga, "Classification of medium resolution satellite imageries using artificial neural network and swarm intelligence," *International Journal of Hybrid Information Technology*, vol. 9, pp. 215–228, 11 2016.

[64] S. L. M. R. Filho, T. A. A. Silva, L. M. G. Vieira, T. H. Panzera, K. Boba, and F. Scarpa, "Geometric effects of sustainable auxetic structures integrating the particle swarm optimization and finite element method," *Materials Research*, vol. 17, pp. 747–757, 3 2014.

[65] U. Singhal and S. Jain, "A new fuzzy logic and gso based load balancing mechanism for public cloud," *International Journal of Grid and Distributed Computing*, vol. 7, pp. 97–110, 10 2014.

[66] N. Chen, W. Liu, R. zhen Bai, and A. Chen, "Application of computational intelligence technologies in emergency management: a literature review," *Artificial Intelligence Review*, vol. 52, pp. 2131–2168, 11 2017.

[67] M. Sood and S. Bansal, "K-medoids clustering technique using bat algorithm," *International Journal of Applied Information Systems*, vol. 5, pp. 20–22, 6 2013.

[68] R. Chandrasekar, R. Suresh, and S. Ponnambalam, "Evaluating an obstacle avoidance strategy to ant colony optimization algorithm for classification in event logs," in *2006 International Conference on Advanced Computing and Communications*, pp. 628–629, IEEE, 2006.

[69] B. Mazzolai, C. Laschi, P. Dario, S. Mugnai, and S. Mancuso, "The plant as a biomechatronic system.," *Plant signaling & behavior*, vol. 5, pp. 90–93, 2 2010.

[70] M. E. Aydin, "Coordinating metaheuristic agents with swarm intelligence," *Journal of Intelligent Manufacturing*, vol. 23, pp. 991–999, 7 2010.

[71] C. E. Torres, L. F. Rossi, J. Keffer, K. Li, and C.-C. Shen, "Modeling, analysis and simulation of ant-based network routing protocols," *Swarm Intelligence*, vol. 4, pp. 221–244, 7 2010.